Accepted for publication to The Astrophysical Journal Letters
Preprint typeset using LaTeX style emulateapj v. 5/2/11

HIGH-ENERGY X-RAYS FROM J174545.5-285829, THE CANNONBALL: A CANDIDATE PULSAR WIND NEBULA ASSOCIATED WITH SGR A EAST

Melania Nynka[1], Charles J. Hailey[1], Kaya Mori[1], Frederick K. Baganoff[2], Franz E. Bauer[3,4], Steven E. Boggs[5], William W. Craig[5,6], Finn E. Christensen[7], Eric V. Gotthelf[1], Fiona A. Harrison[8], Jaesub Hong[9], Kerstin M. Perez[10], Daniel Stern[11], Shuo Zhang[1], and William W. Zhang[12]

Accepted for publication to The Astrophysical Journal Letters

ABSTRACT

We report the unambiguous detection of non-thermal X-ray emission up to 30 keV from the Cannonball, a few-arcsecond long diffuse X-ray feature near the Galactic Center, using the *NuSTAR* X-ray observatory. The Cannonball is a high-velocity ($v_{proj} \sim 500$ km s^{-1}) pulsar candidate with a cometary pulsar wind nebula (PWN) located $\sim 2'$ north-east from Sgr A*, just outside the radio shell of the supernova remnant Sagittarius A (Sgr A) East. Its non-thermal X-ray spectrum, measured up to 30 keV, is well characterized by a $\Gamma \sim 1.6$ power-law, typical of a PWN, and has an X-ray luminosity of $L(3-30 \text{ keV}) = 1.3 \times 10^{34}$ erg s^{-1}. The spectral and spatial results derived from X-ray and radio data strongly suggest a runaway neutron star born in the Sgr A East supernova event. We do not find any pulsed signal from the Cannonball. The *NuSTAR* observations allow us to deduce the PWN magnetic field and show that it is consistent with the lower limit obtained from radio observations.

Subject headings: Galaxy: center ISM: individual (Sagittarius A) - ISM: individual (Sagittarius A East) - ISM: individual (Sagittarius A East) - ISM: supernova remants - stars: neutron - X-rays: individual(Cannonball)

1. INTRODUCTION

Sagittarius A (Sgr A) East is an elongated non-thermal radio shell, which in the west encompasses Sgr A* and Sgr A West, and in the east is bounded by a molecular cloud with which it is likely interacting. The region interior to the radio shell emits thermal X-rays. Park et al. (2005) (hereafter P05), using data from *Chandra* observations, found the X-ray emission comes from three distinct regions: a Center region highly enriched in Fe and other elements; a North region more modestly enriched in Fe; and a 'Plume' region with solar abundances. Each region contains a thermally emitting plasma of temperature ~ 1 keV. The North region contains a higher temperature component with $kT \sim 5-10$ keV. Based on the total Fe abundance, several authors conclude that Sgr A East is likely the result of a Type II supernova (SN) explosion (Maeda et al. 2002; Sakano et al. 2004; Park et al. 2005). However, none of the observations conclusively rule out a Type Ia explosion. The presence of a non-thermal radio shell with no corresponding X-ray emission, along with the center-filled X-ray morphology, argue persuasively that Sgr A East is a mixed morphology supernova remnant (SNR) (Maeda et al. 2002).

Outside the radio shell of Sgr A East, just north of the Plume, lies the *Chandra* source CXOGC J174545.5−285829 (Muno et al. 2003), termed 'the Cannonball.' This source has faint surrounding asymmetric X-ray emission, slightly elongated in the north-south direction, suggesting a cometary tail pointing back to the approximate center of Sgr A East (P05). Based on its non-thermal X-ray emission, spatial extent (~ 0.1 pc at 8 kpc), association with Sgr A East, and lack of flux variation on year time scales, CXOGC J174545.5−285829 has been proposed as a runaway neutron star (NS) with a pulsar wind nebula (PWN). However, due to the lack of spectral coverage above 8 keV, *Chandra* was unable to resolve a high-temperature thermal model, such as what would be found in a cataclysmic variable, from a non-thermal spectrum typical of a PWN. So far, pulsations remain undetected.

The radio observations present a similar picture. A radio counterpart to the Cannonball is detected at 5.5 GHz (Zhao, Morris, & Goss 2013, hereafter ZMG13) that connects to a radio plume region ($\sim 30'' \times 15''$) and a long radio tail ($\sim 30''$) trailing from the radio shell back into the interior of Sgr A East. This morphology is similar to that observed for several runaway NSs (e.g. the Mouse; Gaensler et al. 2004). The proper motion, implying a transverse speed of $\sim 500 \pm 100$ km s^{-1}, flat spectrum ($\alpha = -0.44 \pm 0.08$ for the compact head, $S_\nu \propto \nu^{-\alpha}$) and the cooling linear tail ($\alpha = -1.94 \pm 0.02$; ZMG13) all strongly suggest that the Cannonball is a PWN associated with a NS that has overrun the shell of Sgr A

[1] Columbia Astrophysics Laboratory, Columbia University, New York, NY 10027, USA
[2] Kavli Institute for Astrophysics and Space Research, Massachusetts Institute of Technology, Cambridge, MA 02139, USA
[3] Instituto de Astrofísica, Facultad de Física, Pontificia Universidad Católica de Chile, 306, Santiago 22, Chile
[4] Space Science Institute, 4750 Walnut Street, Suite 205, Boulder, CO 80301, USA
[5] Space Sciences Laboratory, University of California, Berkeley, CA 94720, USA
[6] Lawrence Livermore National Laboratory, Livermore, CA 94550, USA
[7] DTU Space - National Space Institute, Technical University of Denmark, Elektrovej 327, DK-2800 Lyngby, Denmark
[8] Cahill Center for Astronomy and Astrophysics, California Institute of Technology, Pasadena, CA 91125, USA
[9] Harvard-Smithsonian Center for Astrophysics, Cambridge, MA 02138, USA
[10] Columbia University, New York, NY 10027, USA
[11] Jet Propulsion Laboratory, California Institute of Technology, Pasadena, CA 91109, USA
[12] NASA Goddard Space Flight Center, Greenbelt, MD 20771, USA

Table 1
NuSTAR Log of Cannonball Observations

ObsID	Start Date (UTC)	Exposure (ks)	Target
30001002001	2012 07 20	166.2	Sgr A*
30001002003	2012 08 04	83.8	Sgr A*
30001002004	2012 10 16	53.6	Sgr A*
80002013002	2013 04 27	54.1	Magnetar ToO
80002013004	2013 05 04	42.1	Magnetar ToO
80002013006	2013 05 11	35.6	Magnetar ToO
80002013012	2013 06 14	29.1	Magnetar ToO

Note. — The exposure times listed are corrected for good time intervals.

East.

Here we report the *NuSTAR* discovery of non-thermal X-rays from the Cannonball up to energies 30 keV. In §2 we describe the *NuSTAR* observations. In §3, §4 and §5 we present the imaging, spectral and timing analysis, respectively. In §6, we use *NuSTAR* and *Chandra* data to estimate the PWN magnetic field strength independent of the lower limit derived from the radio observations of ZMG13.

2. *NuSTAR* OBSERVATIONS

NuSTAR is the first focusing telescope that operates in the hard X-ray band of $10-79$ keV. It consists of two coaligned optics/detector pairs, focal plane modules A and B (FPMA and FPMB), and has a field of view of $10' \times 10'$ at 10 keV. *NuSTAR* has an angular resolution of $18''$ full width at half maximum (FWHM) and $58''$ half power diameter, and an energy resolution of 400 eV (FWHM) at 10 keV (Harrison et al. 2013). The nominal *NuSTAR* timing resolution is 4 ms. The nominal *NuSTAR* reconstruction coordinates are accurate to $8''$ (90% confidence level). In the following study, all observation were processed using *nupipeline*, NuSTARDAS v. 1.1.1, which is used to generate response matrices and exposure maps, and the HEASoft v. 6.13 package is used for data analysis.

NuSTAR observed Sgr A* three times between 2012 July 20 and 2012 October 10 (Barrier et al. 2013). In addition, *NuSTAR* triggered multiple target of opportunity observations(ToO), four of which were used in the subsequent analysis, of the outburst from the newly-discovered magnetar SGR J1745-29 near Sgr A* in 2013 (Mori et al. 2013). The Cannonball, located $\sim 2'$ away from Sgr A*, was captured in the *NuSTAR* field of view in all seven observations, with a total exposure time of 429 ks (Table 1). We performed imaging and spectral analysis using the three Sgr A* observations, as the Cannonball falls on or near the detector chip gaps in the SGR J1745−29 observations, which were otherwise suitable for timing analysis. Photon arrival times were corrected for on-board clock drift and precessed to the solar system barycenter using the JPL-DE200 ephemeris and the *Chandra* subarcsec position (P05).

3. IMAGING ANALYSIS

We applied astrometric corrections to each *NuSTAR* event file by aligning *NuSTAR*-detected objects with their reference *Chandra* locations (Muno et al. 2003). This is particularly important in the crowded Galactic Center region as it increases the significance of faint sources. We then generated a mosaiced *NuSTAR* image of the Cannonball by merging exposure-corrected images from each observation. The resulting $3-79$ keV mosaic is shown in Figure 1, along with the $3-8$ keV *Chandra* contours (P05). It is clear that the *Chandra* contours are centered on the bright Cannonball emission in the *NuSTAR* image. The $10-30$ keV *NuSTAR* image is shown as an inset. The Cannonball is detected as an isolated source at energies above 10 keV. Above 30 keV the source becomes background-dominated, and below 10 keV the source is too faint to be detected over thermal emission from the Plume region and Sgr A East, which contribute due to the *NuSTAR* PSF.

We investigated whether the Cannonball exhibits any elongation above 10 keV as observed in the radio band (ZMG13). First, we generated an effective PSF by taking into account the appropriate off-axis angle and orientation for each observation then adding individual PSFs weighed by exposure time. Second, we used the effective PSF to convolve a 2-D Gaussian model profile to fit a circular region with $30''$ radius around the Cannonball using `Sherpa`, a CIAO modeling and fitting application (Fruscione et al. 2006). The best-fit centroid position of the Cannonball overlaps the *Chandra* position within the position uncertainty of $3.3''$ (90% confidence). The best-fit FWHM=$3.0'' \pm 2.7''$ shows that the Cannonball is not resolved by *NuSTAR*. Additionally, we analyzed residuals of the 2-D image by fitting along various axes through the Cannonball, and did not find any elongation of the source within statistical uncertainties. We cannot detect the small $\sim 2''$ tail observed by *Chandra* (P05).

4. SPECTRAL ANALYSIS

We extracted source spectra from the three *NuSTAR* Sgr A* observations using a $20''$ radius circular region centered on the *Chandra* position (white circle in Figure 1). This region is optimal for spectral analysis since it significantly reduces the contribution of the nearby Plume and Sgr A East emission, indicated in Figure 1, and maximizes the signal-to-noise ratio. After rebinning *NuSTAR* spectra to > 20 counts per bin, we performed spectral fitting with `XSPEC` version 12.8.0 (Arnaud 1996) and adopted the abundance and atomic cross-section data from Wilms et al. (2000) and Verner et al. (1996), respectively. Due to the broad *NuSTAR* PSF, this source extraction region will also contain thermal emission from the Sgr A East Plume and North regions. The *NuSTAR* spectrum can therefore be fit with an absorbed thermal and non-thermal model, **Tbabs*(apec+powerlaw)**.

NuSTAR background spectra were extracted from partial annuli shown in Figure 1 (green dashed region). These regions were chosen to remove instrument and cosmic X-ray background, as well as the contribution of point sources detected by *Chandra* (Muno et al. 2003). These sources, which are too faint to be detected by *NuSTAR* individually, collectively add an additional background component. Muno et al. (2003) used *Chandra* to resolve these point sources and determined that they were peaked at the Galactic Center and decrease radially from Sgr A* outward. We therefore chose background regions at the same radial distance from Sgr A* as the Cannonball, and avoided the known filaments, Sgr A East and detector chip gaps.

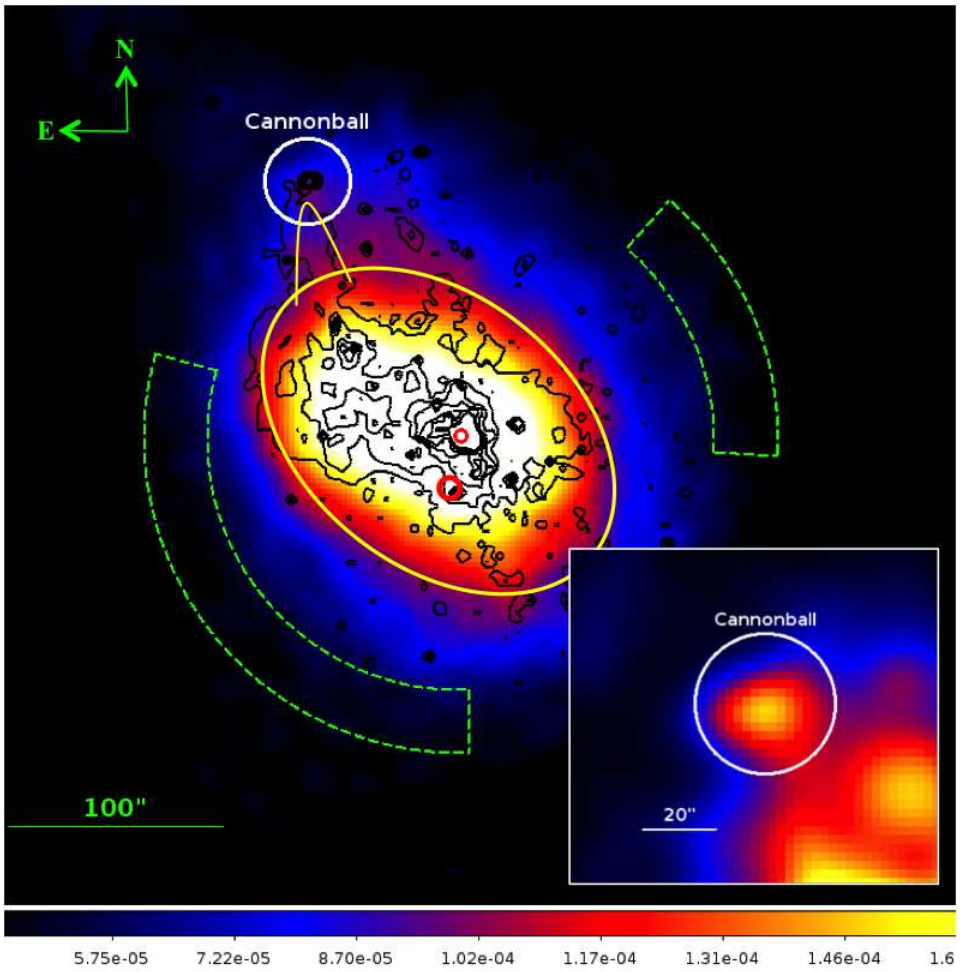

Figure 1. *NuSTAR* mosaic image of the Cannonball, Plume, and SgrA* region in $3-79$ keV band. The Cannonball is indicated by the white circle with radius of $20''$. Background regions are indicated by the green dashed regions. *Chandra* $3-8$ keV contours are overlaid in black, and approximate positions of the Plume and SgrA East are in yellow. The image is shown with a linear color scale and the scale range chosen to highlight the Cannonball emission. Inset– *NuSTAR* mosaic image of the Cannonball in $10-30$ keV band.

We used data from *Chandra* ACIS-I to constrain the column density. The *Chandra* spectrum was obtained from 82 ACIS-I observations, spanning from 2000 October to 2012 October, with a total integration time of 4 Ms. We used a source region $r = 1.6''$ to remove contamination from the adjacent soft foreground star, CXOGC J174545.2-285828, which has a thermal spectrum negligible above 2 keV (P05) and does not affect *NuSTAR* spectra. The *Chandra* background spectra were extracted from a region adjacent to the Cannonball, in order to subtract thermal emission from the Plume and Sgr A East. The *Chandra* spectrum can be fit with an absorbed power-law model, **Tbabs*powerlaw**.

We then jointly fit the *NuSTAR* and *Chandra* data. The absorption coefficient and the power-law parameters were linked between the two data sets. We analyzed the *NuSTAR* spectra in $3-30$ keV and *Chandra* data in $2-8$ keV. The fit results are shown in Figure 2 and Table 2. The best-fit power-law photon index is $\Gamma = 1.6 \pm 0.4$, consistent with the *Chandra* results of P05. The discrepancy between the best-fit absorption column and that found in P05 is due to our use of more recent absorption and abundance data.

As an alternative approach, we restricted the *NuSTAR* data to the $13-30$ keV band to cleanly isolate the non-thermal Cannonball emission from the low-temperature thermal components of the Sgr A East Plume and North regions. We then jointly fit *NuSTAR* and *Chandra* spectra with an absorbed power-law model for both spectra, with all parameters linked. The best-fit parameters for the power-law model, shown in Figure 2 and Table 2, are consistent with the values found in the full-band spectral analysis.

Table 2
Results from NuSTAR + Chandra joint spectral analysis

Parameters	Power-law+Apec	Power-law
NuSTAR Energy Band [keV]	$3-30$	$13-30$
$N_{\rm H}[10^{22}\,{\rm cm}^{-2}]$	31^{+2}_{-3}	32^{+2}_{-3}
Power-law Index	$1.6^{+0.3}_{-0.4}$	$1.6^{+0.4}_{-0.3}$
kT [keV]	2.8 ± 0.1	···
χ^2_ν [dof]	0.81 (66)	0.90 (39)
$F_{\rm X}(2-10$ keV)	7 ± 3	7 ± 2
$F_{\rm X}(10-30$ keV)	9^{+2}_{-3}	9 ± 1

Note. — Best-fit parameters of the Cannonball, joint fit *NuSTAR* and *Chandra* data. The errors are 90% confidence level. Flux values are obtained from the power-law component, and have units $10^{-13}\,{\rm erg\,s^{-1}\,cm^{-2}}$.

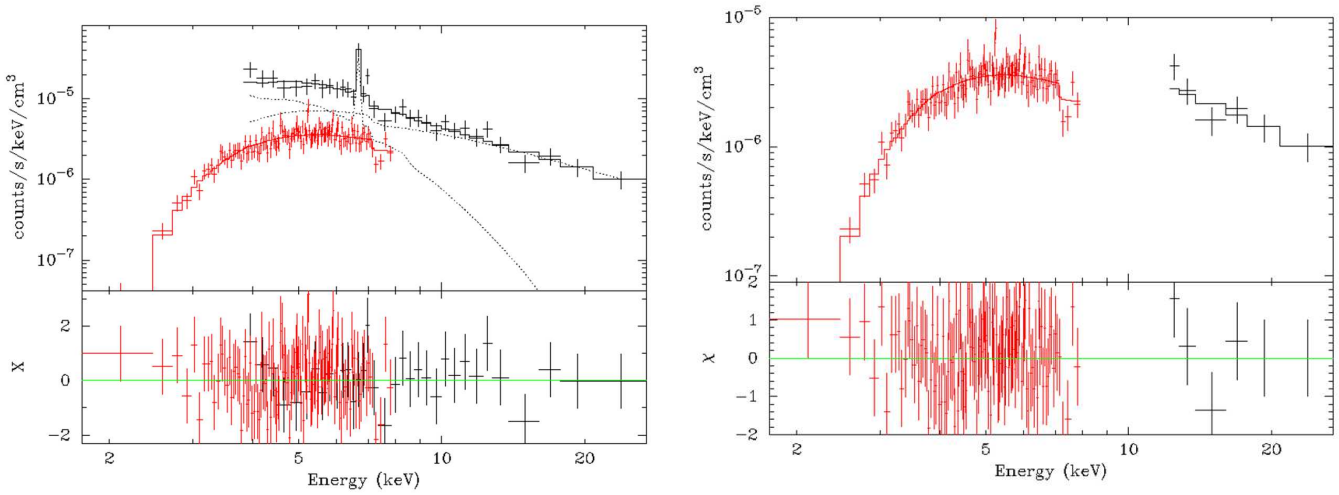

Figure 2. Cannonball joint fit with *NuSTAR* and *Chandra*. Left– 2-30 keV joint fit. Solid lines are the best-fit model. Dashed lines are the model components (thermal, and non-thermal) of the *NuSTAR* data. Right– Cannonball-only spectral fit with an absorbed power-law model. For both images, black indicates *NuSTAR* FPMA data, red indicates *Chandra ACIS* data.

5. TIMING ANALYSIS

The high time resolution of *NuSTAR* allows a search for pulsations down to periods of $P = 4$ ms, covering the expected range for a rotation powered pulsar. Previous searches were restricted to $P > 147$ ms (P05). We evaluated the power at each frequency (oversampling by a factor of 2) using the Z_n^2 test statistic for $n = 1, 2, 3, 5$, to be sensitive to both broad and narrow pulse profiles. We initially restricted the timing search to photons energies in the $3 - 25$ keV range and used an aperture of $20''$ to optimize the signal-to-noise ratio.

From a search of all the observations, the most significant signal was $Z_3^2 = 48.61$ for ObsID 30001002001, corresponding to a probability of false detection of $\wp = 0.25$ for $28 \times (8.9 \times 10^9)$ search trials. The resulting period is not reproduced in the other observations. We repeated our search for an additional combination of energy ranges $3 < E < 10$ keV, $10 < E < 25$ keV and aperture size $r < 10''$. We also searched the combined data set in $(f, \dot{f})$-space around our best candidates from the individual observations. None of these resulted in a significant detection. We conclude that no pulsed X-ray signal is detected from the Cannonball. After taking into account the estimated background emission (except for PWN contribution) from §4, we place an upper limit on the pulse fraction at the 99.73% confidence level (3σ) of $f_p \leq 43\%$ for a sinusoidal signal in the $3 - 25$ keV band for the $r < 20''$ aperture.

6. DISCUSSION

6.1. *Is the Cannonball a Pulsar?*

NuSTAR observations of the Cannonball establish the existence of a non-thermal power-law component extending up to $\sim$ 30 keV. The joint fit to the *NuSTAR* – *Chandra* spectrum shows a single power law with a photon index of $\Gamma = 1.6$ extending from 2 keV to $\sim$ 30 keV. Furthermore, the > 10 keV X-rays are coincident to $\sim 3''$ with the central point-like head of the cometary structure detected by *Chandra*. This is fully consistent with expectations from a PWN. The highest energy X-rays are associated with the highest energy electrons – the ones which cool most quickly downstream from the termination shock. Given that the soft X-rays detected by *Chandra* are emanating from a region of $\sim 2''$, one expects the emission above 10 keV to be from an even smaller region. Indeed this is consistent with the *NuSTAR* detection of an unresolved point source, localized on the centroid of the soft X-ray emission. Thus the cometary soft X-ray morphology and point-like hard X-ray emission are consistent with a bulk velocity field cooled by synchrotron emission – a PWN.

Further support for a PWN origin for the Cannonball comes from the radio observations (ZMG13), where a cometary morphology is also detected, along with an extended plume and tail region consistent with a ram pressure-confined outflow. ZMG13 also point out the similarity of the head-tongue structure with the Mouse PWN. Moreover, the hardening of the radio spectrum downstream from the head-tongue structure is indicative of a cooling outflow downstream from a termination shock.

The non-thermal energy spectrum for the head region of the Cannonball exhibits a steepening of $\Delta\alpha = \alpha_x - \alpha_r = 0.9 \pm 0.5$, with $\alpha_x = \Gamma - 1$. This is comparable within uncertainties to the classic case of a 0.5 break in the radio-X-ray spectrum, which is the spectral steepening associated with the continuous injection of electrons into a homogeneous source cooled by synchrotron losses. Further support for the PWN identification comes from the transverse velocity measured by ZMG13. Previous work (Maeda et al. 2002; Sakano et al. 2004; Park et al. 2005) all propose a Type II SN event as a likely origin for Sgr A East, and the ~ 500 km s^{-1} transverse velocity is consistent within expectations for Type II SNe, where high pulsar ejection velocities are expected.

Neither radio nor *NuSTAR* searches turn up any pulsation. It is very rare to detect radio pulsars near the Galactic Center due to interstellar dispersion (Deneva et al. 2009). Additionally, the Cannonball sits in a region of high X-ray background making detection of X-ray pulsations difficult. Our pulsed fraction upper limit of 43% indicates that the Cannonball has a spin period shorter than 4 ms or its pulsar emission is buried under the bright PWN emission. Our result extends

the range of non-detection from 147 ms (P05) to 4 ms. In several young PWNe (e.g. G21.5-0.9, Nynka & et al. (2013)), pulsar emission remains undetected in the X-ray band due to significantly brighter PWN emission. Therefore, the non-detection of pulsations from the Cannonball is not surprising.

Some PWN, such as G21.5-0.9, exhibit strong γ-ray emission detectable with HESS (H. E. S. S. Collaboration et al. 2007). Inverse-Compton emission for the Cannonball was predicted using a model by Zhang et al. (2008), incorporating an appropriate IR flux (Hinton & Aharonian 2007). Based on the diffuse γ ray emission in the Galactic Center (Viana 2011), the Cannonball would either have marginal or no detection by HESS.

6.2. *Magnetic Field of the Cannonball PWN*

An estimate of the PWN magnetic field can be obtained from the *NuSTAR* and *Chandra* data. We assume a constant (mean) magnetic field and a bulk flow velocity field downstream of the termination shock of the form $v(r) = c/3(r_s/r)^2$ where r_s is the termination shock radius. These are approximations to the exact solution of Kennel & Coroniti (1984). Integrating this equation we obtain $r_l(E) = (cr_s^2\tau)^{1/3}$. We assume $r_l \gg r_s$, (which the results below confirm). X-ray emission ceases at downstream distance $r_l(E)$, and $\tau(E)$ is the timescale for synchrotron cooling of electrons emitting X-rays of characteristic energy E. Normally the termination shock radius is estimated by balancing the pressure of the relativistic wind with the ram pressure of the ISM (Gaensler & Slane 2006). However,since the Cannonball moves through the hot plume region of Sgr A East, we add an additional term for the thermal pressure so that $\dot{E}/4\pi r_s^2 c\omega = \rho v^2 + P_{th}$ where $\dot{E}$ is the pulsar spindown power, ρ the density of the ISM, v the pulsar space velocity and ω a fill factor for the pulsar wind. P05 assume that the Cannonball outflow is energizing the plasma observed in the Plume region. Thus the Plume's X-ray emitting plasma provides a direct measure of the ISM density, n, through which the Cannonball is moving. From P05 one derives this ISM density for the Plume of $n \sim 9$ cm$^{-3} f^{-1/2}$, where f is the plasma volume filling factor. The thermal pressure of the Plume was given in P05, and we convert this to an effective thermal velocity, $P_{th} = \rho v_{th}^2 (v_{th} = 465$ km s$^{-1})$. The $\dot{E}$ for the pulsar cannot be obtained directly, since no pulsations were detected (§5). However, Gotthelf (2003) provides an empirical formula relating $\dot{E}$ to the measured photon index, $\Gamma = 2.36 - 0.021\dot{E}_{40}^{-1/2}$. Using the *NuSTAR* derived photon index yields $\dot{E} = 7 \times 10^{36}$ erg s^{-1} (Table 3).

With the above estimates the termination shock radius is $r_s = 0.006\mathrm{pc}(1 + (v/465)^2)^{-1/2} f^{1/4}\omega^{-1/2}$, where v is the pulsar space velocity in km s^{-1}. Using the cooling time scale, a function of magnetic field strength B and characteristic energy E (Ginzburg & Syrovatskii 1965), one can solve the cooling length scale equation to obtain $B = 884\mu\mathrm{G}(1 + (v/465)^2)^{-2/3} f^{1/3}\omega^{-2/3}$. The cooling length scale used to derive the magnetic field was estimated from the $3-8$ keV *Chandra* image of P05, assuming the maximum extent of the image was associated with the (slowest cooling) 3 keV X-rays ($r_l = 0.03$ pc). The 500 km s^{-1} transverse velocity obtained by ZMG13 is a lower limit on the pulsar space velocity. Approximately 90% of all pulsars have space velocities less than 900 km s^{-1} (Arzoumanian et al. 2002), so using these velocities as an approximate range, one obtains $r_s \sim (0.003 - 0.005)\mathrm{pc} f^{1/4}\omega^{-1/2}$, consistent with estimates of the termination shock radius for other PWN. The magnetic field is $B \sim (313{-}530)\,\mu\mathrm{G}\, f^{1/3}\omega^{-2/3}$. The magnetic field estimate is in excellent agreement with the lower limit of $B > 300\ \mu$G obtained by ZMG13 for the Cannonball head assuming energy equipartition.

Table 3
Cannonball Properties

Parameters	Value
$L_x(2-10$ keV) [erg s^{-1}]	$6^{+2}_{-3} \times 10^{33}$
$L_x(10-30$ keV) [erg s^{-1}]	$7 \pm 1 \times 10^{33}$
$\dot{E}$ [erg s^{-1}]	$\sim 7 \times 10^{36}$
r_s [pc]	$\sim 0.003 - 0.005$
B(PWN) [μG]	$\sim 313 - 530$
B(NS) [G]	$\sim 5 \times 10^{12}$

Note. — Best-fit parameters of the Cannonball, joint fit with *NuSTAR* and *Chandra* data. The errors are 90% confidence level. Flux values are obtained from the power law component of the *NuSTAR* data. Line-of-sight distance to the Cannonball is assumed to be 8kpc.

6.3. *Magnetic Field of the Putative Pulsar*

Assuming a magnetic braking index of 3 and an initial spin period $P_o \ll P$, where P is the current spin period, an expression for the NS surface magnetic field strength can be obtained by (very approximately) assuming that the pulsar characteristic age is equal to the observed age τ: $B = 3.2\times10^{19}$ G $(\pi^2 I/\tau^2\dot{E})^{1/2}$ (Manchester & Taylor 1977). Using the $\dot{E}$ derived above, a pulsar age of 9000 ± 100 yr, and assuming $I = 10^{45}$ g cm^2 for a NS of $1.4M_\odot$ and $R = 10$ km, we obtain $B \sim 5 \times 10^{12}$ G.

7. SUMMARY

The Cannonball has been detected by *NuSTAR* at energies up to $\sim$ 30 keV, revealing the presence of non-thermal emission. This observation, combined with the recent discovery of proper motion of the Cannonball with speed $\sim$ 500 km s^{-1} and direction pointing towards the center of the Sgr A East SNR, further solidifies the case that the Cannonball is the NS associated with Sgr A East. A timing search for pulsation was unsuccessful. An estimate of the PWN magnetic field from the X-ray data is consistent with a lower limit obtained from radio data by equipartition arguments.

This work was supported under NASA contract No. NNG08FD60C, and made use of data from the *NuSTAR* mission, a project led by the California Institute of Technology, managed by the Jet Propulsion Laboratory, and funded by the National Aeronautics and Space Administration. We thank the *NuSTAR* Operations, Software and Calibration teams for support with the execution and analysis of these observations. This research has made use of the *NuSTAR* Data Analysis Software

(NuSTARDAS) jointly developed by the ASI Science Data Center (ASDC, Italy) and the California Institute of Technology (USA). The authors wish to thank Jules Halpern for useful discussions.

REFERENCES

Arnaud, K. A. 1996, in Astronomical Society of the Pacific Conference Series, Vol. 101, Astronomical Data Analysis Software and Systems V, ed. G. H. Jacoby & J. Barnes, 17
Arzoumanian, Z., Chernoff, D. F., & Cordes, J. M. 2002, ApJ, 568, 289
Barrier, N., Tomsick, J. A., Baganoff, F. K., & Boggs, S. E. 2013, ApJ, submitted for publication
Deneva, J. S., Cordes, J. M., & Lazio, T. J. W. 2009, ApJ, 702, L177
Fruscione, A., McDowell, J. C., Allen, G. E., et al. 2006, in Society of Photo-Optical Instrumentation Engineers (SPIE) Conference Series, Vol. 6270, Society of Photo-Optical Instrumentation Engineers (SPIE) Conference Series
Gaensler, B. M., & Slane, P. O. 2006, ARA&A, 44, 17
Gaensler, B. M., van der Swaluw, E., Camilo, F., et al. 2004, ApJ, 616, 383
Ginzburg, V. L., & Syrovatskii, S. I. 1965, ARA&A, 3, 297
Gotthelf, E. V. 2003, ApJ, 591, 361
H. E. S. S. Collaboration, :, Djannati-Atai, A., et al. 2007, ArXiv e-prints, arXiv:0710.2247
Harrison, F. A., Craig, W. W., Christensen, F. E., et al. 2013, ApJ, 770, 103
Hinton, J. A., & Aharonian, F. A. 2007, ApJ, 657, 302
Kennel, C. F., & Coroniti, F. V. 1984, ApJ, 283, 710
Maeda, Y., Baganoff, F. K., Feigelson, E. D., et al. 2002, ApJ, 570, 671
Manchester, R. N., & Taylor, J. H. 1977, San Francisco : W. H. Freeman, c1977., 36
Mori, K., Gotthelf, E. V., Zhang, S., et al. 2013, ApJ, 770, L23
Muno, M. P., Baganoff, F. K., Bautz, M. W., et al. 2003, ApJ, 589, 225
Nynka, M., & et al. 2013, ApJ, submitted for publication
Park, S., Muno, M. P., Baganoff, F. K., et al. 2005, ApJ, 631, 964
Sakano, M., Warwick, R. S., Decourchelle, A., & Predehl, P. 2004, MNRAS, 350, 129
Verner, D. A., Ferland, G. J., Korista, K. T., & Yakovlev, D. G. 1996, ApJ, 465, 487
Viana, A. 2011, in SF2A-2011: Proceedings of the Annual meeting of the French Society of Astronomy and Astrophysics, ed. G. Alecian, K. Belkacem, R. Samadi, & D. Valls-Gabaud, 621–625
Wilms, J., Allen, A., & McCray, R. 2000, ApJ, 542, 914
Zhang, L., Chen, S. B., & Fang, J. 2008, ApJ, 676, 1210
Zhao, J.-H., Morris, M. R., & Goss, W. M. 2013, ApJ, submitted for publication